Ab Initio Study of Free-Radical Polymerization: Defect Structures in Poly(vinyl chloride)

Karen Van Cauter, Bart J. Van Den Bossche,† Veronique Van Speybroeck,* and Michel Waroquier

Center for Molecular Modeling, Ghent University, Proeftuinstraat 86, B-9000 Ghent, Belgium

Received September 19, 2006; Revised Manuscript Received December 5, 2006

ABSTRACT: The main reaction routes that lead to the formation of structural defects in PVC are studied on a theoretical basis with the BMK/6-311+G(3df,2p)//B3LYP/6-31+G(d) method. All studied reactions can be classified into four classes: the reactions following a head-to-head addition, intramolecular H-transfer (backbiting), and chain transfer reactions to polymer and to monomer. The head-to-tail propagation is the reference reaction for estimating the probability of the reaction routes leading to defect formation. Variations of chain length of the reacting polymer chain were taken into account in the calculations, leading to more than 100 studied reactions. The ab initio kinetic parameters, combined with typical monomer and polymer concentrations during suspension polymerization, serve as an input for the calculation of the defect concentrations that can be compared to the experimental data. This work supports the overall mechanism of defect formation during vinyl chloride polymerization as established experimentally.

1. Introduction

Poly(vinyl chloride) (PVC) is the second most produced plastic in the world (>30 Mton/year), placing it after polyolefins but before styrene polymers.[1] The industrial production proceeds mainly via the heterogeneous process of suspension polymerization. The structural defects in PVC, such as the tertiary chlorines at branched carbons, allylic chlorines (adjacent to internal unsaturations), oxygen containing groups, end groups, ..., are of practical importance despite their low concentrations, since they affect the color, thermal stability, crystallinity, processing, and mechanical properties of the finished materials.[2] In particular, the susceptibility of PVC toward thermal degradation is a point of interest, since the thermal instability of PVC is far more pronounced than that of other important thermoplastics (such as polystyrene and polymethyl methacrylate). More details about the structural and mechanistic aspects of the thermal degradation of PVC can be found in a recent review of Starnes.[3] This problem is circumvented by adding thermal stabilizers to the finished polymer during compounding operations, which however have a strong negative influence on the environment. Further insights into the formation of the defect structures is thus desirable with the final aim to suggest alternative ways of stabilizing PVC. The labile defect structures have been extensively investigated by both chemical and spectroscopic methods. Nowadays, it is believed that tertiary chlorine and internal unsaturations are the most important labile defects in PVC. The former structure is associated with the butyl branches and with a major part of the long chain branches.[3−6] Recently Starnes published a review of his research on defect structures in PVC performed over the last 30 years.[7] This work has led to the identification and quantification of the anomalous structures in PVC and the detailed descriptions of their mechanisms of formation. Xie et al. and Hjertberg et al. also did a lot of experimental efforts to elucidate the mechanisms of defect formation in PVC.

Structural defects in PVC have been measured mainly by NMR techniques by the IUPAC working party devoted to that subject. The typical defect structure concentrations reported in literature are summarized in Table 1. The most abundant side chain structures are the methyl branches with tertiary hydrogen (MB, 3.3−4.8/1000 VC), followed by the butyl branches (BB, 0.5−1.7/1000 VC) carrying tertiary chlorine. The concentration of long chain branches (LCB with tertiary Cl and LCB′ with tertiary H) and 1,2-dichloroethyl branches (EB) is an order of magnitude lower, while the concentrations of pentyl branches (PB) and diethyl branches (DEB) are below the detection limit (i.e., < 0.1/1000 VC), as well as the concentrations of potential methyl branches and 1-chloro-ethyl branches with tertiary chlorine (MB′ and EB′). The most abundant unsaturated end group is the 1-chloro-2-alkene end group (EA, allylic end group, 0.45−0.95/molecule), the most abundant saturated end group is the 1,2-dichloroalkane end group (LE′, 0.8−0.9/molecule). The 1,3-dichloroalkane (LE) end group also occurs but at a lower concentration than the LE′ end group. The internal double bond content (IA) is about 0.0−0.6/1000 VC. It has been shown that the sums of the concentrations of EA and IA structures are always very close to 1.0 per polymer molecule.[8]

Xie et al. have established a correlation between the concentration of tertiary chlorine atoms and the dehydrochlorination rate d[HCl]/d*t*, and have argued that the tertiary chlorine (found at branching points in PVC) is probably the defect structure that is most responsible for the reduced thermal stability of PVC. Also internal double bonds have been measured but their concentration is a factor of 10 lower and no clear relationship was found with d[HCl]/d*t*.[6] However the techniques used by Hjertberg and others to measure internal unsaturation have been criticized, and the same is true for other chemical methods and the earlier NMR techniques, including those of the IUPAC working party. This situation is reviewed in ref 8, which argues that the use of high-field proton NMR is the only reliable approach to the quantitative determination of both internal and terminal double bonds. Most researchers now believe that both tertiary chlorine and the IA structure

* Corresponding author. Fax: (+32)9-264-6697. E-mail: Veronique.Vanspeybroeck@UGent.be.

† Current address: BASF Antwerpen N.V., Haven 725, Scheldelaan 600, B-2040 Antwerpen 4, Belgium.

10.1021/ma062174s CCC: $37.00
Published on Web 01/26/2007

Table 1. Experimental Concentrations of Structural Defects in PVC, in Number per 1000 VC Units, Where the Results Are Obtained by NMR Techniques (^{1}H and ^{13}C)

	type defect	experimental range	references
MB	chloromethyl branch (tertiary H)	3.3−4.8	3.8−4.4,[4] 3.3−4.8,[5] 4.5,[9] 3.8[41]
BB	2,4-dichloro-*n*-butyl branch	0.5−1.7	0.5−1[a],[4] 0.50−1.7,[5] 1.5,[9] 0.7−0.9,[22] 0.9−1.25,[39] 0.8[41]
EA	1-chloro-2-alkene end group	0.45−0.95[b]	0.7[b],[4] 0.4−0.8,[8] 0.45[b],[9] 0.85−0.95[b],[12] 0.75[41]
LE'	1,2-dichloroalkane end group	0.8−0.9[b]	0.8−0.9[b] [4]
EB	1,2-dichloroethyl branch	0.14−0.55	0.14−0.55,[5] 0.4,[9] 0.4[42]
IA	internal allylic bond	0.0−0.6	0.08−0.15;[c] 0.05−0.15[d],[5] 0.08−0.11,[6] 0.0−0.6,[8] 0.4−0.45,[9] 0.1−0.2,[37] 0.1−0.3;[c] 0.45[d],[41]
LCB	long chain branch (tertiary Cl)	0.07−0.14	2/3 of ([LCB]+[LCB′])[4]
LCB'	long chain branch (tertiary H)	0.03−0.07	1/3 of ([LCB]+[LCB′])[4]
LCB+LCB'	long chain branch	0.1−0.2	0.11−0.20,[5] 0.1[41]
LE	1,3-dichloroalkane end group	<0.75[e]	
DEB	1,3-bis(2-chloroethyl) branch	ND	only observed at low monomer pressures[40]
MB'	chloromethyl branch (tertiary Cl)	ND	
EB'	ethyl branch (tertiary Cl)	ND	only observed at high temp[7]
PB	pentyl branch	ND	

[a] Includes also the LCB concentration but this is a minor contribution. [b] The end group structures EA and LE′ are expressed in number per molecule. [c] By ozonolysis. [d] From ^{1}H NMR. [e] The value of 0.75 from ref 25 is an overestimation since hydrogen abstraction from cyclohexane produced most of the LE ends in the studied polymer. (ND = Not Detected.)

make important contributions to the thermal instability of PVC.[3,9]

The extensive research on PVC polymerization reflects the enormous interest in the subject. A lot of experimental data are available concerning the polymerization kinetics. Some averaged rate constants for the main polymerization steps (initiation, propagation, chain transfer,...) have been derived by regression of experimental data for the monomer conversion and molecular mass distribution as a function of reaction time and temperature.[10−12] Nevertheless, a comprehensive kinetic model which can accurately predict all properties of the synthesized polymer is still lacking due to the complexity of the polymerization process. In this respect ab initio calculations on individual reaction steps can improve the fundamental insight into the polymerization, since all effects can be studied separately and the relative importance of concurrent reactions can be estimated. Theoretical chemistry has been often applied in the field of polymer chemistry during the past decade by several research groups (Radom et al.,[13−15] Gilbert et al.,[16−18] Coote et al.[9,19]), but despite this the number of modeling studies on PVC polymerization is rather limited. Recently, a combined experimental and theoretical work was published by Purmova et al. concerning the effect of monomer conversion on the nature and concentration of structural defects in radical suspension polymerization of vinyl chloride. Some elementary reaction steps were modeled to explain trends in measured defect concentrations at high monomer conversion.[9] Also recently Izgorodina and Coote have proposed a systematic methodology for calculating propagation rate constants of acrylonitrile and vinyl chloride, taking into account effects of solvent and chain length of the polymer.[19] In the current work, the effect of chain length was also properly taken into account. Previously, we already investigated this item for the propagation of polyethylene[20] and also Heuts has addressed this item in ref 21.

The principal aim of this work is to study all elementary reaction steps that give rise to anomalous structures in PVC. To this end, a reaction network is introduced that ties together the most important reaction steps leading to defects. Basically, five different reaction classes can be distinguished, as schematically presented in Scheme 1. The normal head-to-tail propagation (reaction class A) is competed by a number of alternative reaction routes (reaction classes B−E) that produce irregular structures. The kinetic parameters of all proposed reaction routes are determined on an ab initio basis. Since the reaction network

Scheme 1. Possible Reaction Pathways during PVC Polymerization, Leading to a Number of Important Defect Structures

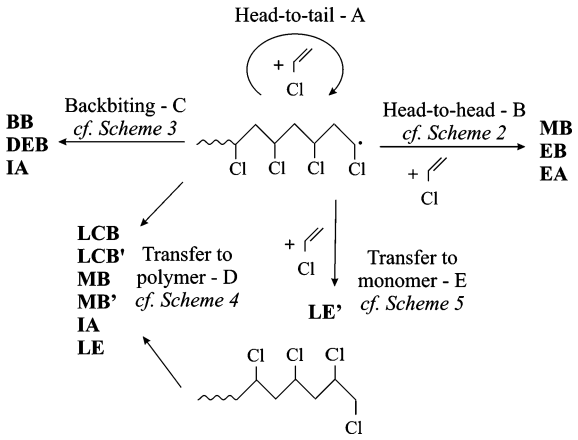

contains both bimolecular and unimolecular reactions, it is not possible to compare directly the rate constants of the elementary reaction steps. Therefore, typical concentrations of monomer and radical during suspension polymerization are taken into account. The latter process is the most common process in the PVC industry and is known to give rise to lower concentration of unsaturations and branches than solution polymerization.[22] The final validation of the network consists of the prediction of the concentration of defect structures at normal conversion. Possible alternative reaction routes that come into play at higher conversions are not taken into account. The oxygenated structures coming from the byproducts of the reactions of accidental traces of oxygen are not considered. Also initiator residues will not be considered in the calculations, since most of the chain end structures are formed through chain transfer to monomer (reinitiation).[3] Diffusion effects are not accounted for as those might come into play only in the polymer rich phase at high monomer conversions.[9]

The current work is organized as follows: in section 2 the reaction mechanisms as schematically represented in Scheme 1 are discussed in detail. Section 3 highlights the methodology for the ab initio calculation of the reaction rates and defect concentrations while section 4 is dedicated to the interpretation of the ab initio data (Results and Discussion). Section 5 summarizes the main conclusions of this work.

Scheme 2. Reaction Class B: Reactions Following Head-to-head Propagation[3,7,9,24,25]

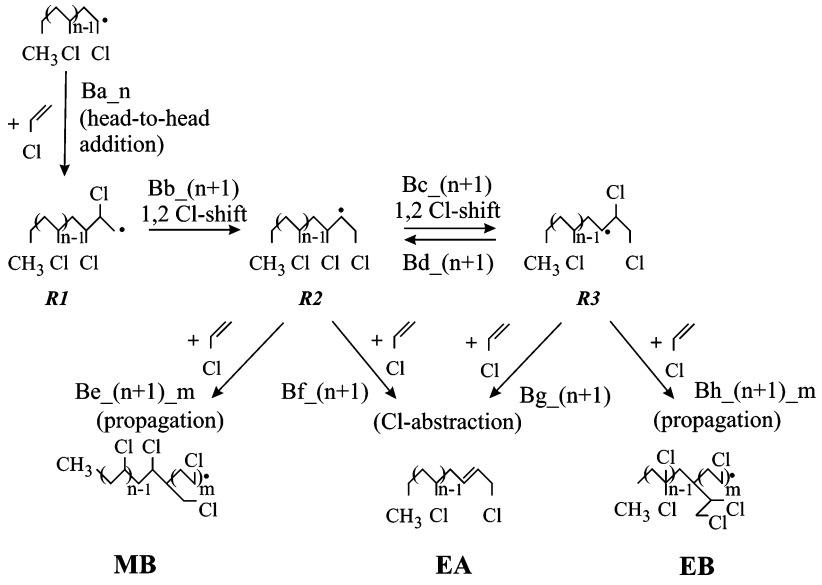

2. Detailed Reaction Mechanisms

Reaction Class A: Head-to-Tail Propagation. The process of free radical polymerization consists of four main reaction steps: initiation, propagation, chain transfer to monomer, and termination. Since we do not aim to describe defects arising from initiator fragments, the radical chain is terminated by a methyl radical in all proposed reaction schemes. This approach is validated since the IUPAC working party has reported that the chain end structure of PVC derived from initiator is negligible, indicating that chain transfer to monomer is predominant.[23] The propagation takes place mainly by head-to-tail addition of the growing radical to the monomer (VC). Exclusive head-to-tail additions would yield a perfectly regular PVC structure. The kinetic parameters of the propagation serve as a reference to estimate the importance of the reactions leading to structural defects (reaction classes B−E).

Reaction Class B: Head-to-Head Propagation. A first competitive mechanism is the head-to-head propagation of the living radical (Scheme 2) and results in the production of methyl branches (MB), ethyl branches (EB) and allylic end groups (EA). The parameter *n* which is taken up in the reaction scheme indicates the number of monomer units in the living radical; e.g. **Ba_1** starts from a radical composed of a CH_3 group with one added monomer unit. The kinetic parameters will be evaluated in terms of varying numbers of *n*. After a head-to-head addition a very reactive radical **R1** is formed which is expected to undergo rapidly a 1,2-Cl shift (**Bb**) toward the radical **R2**. Propagation from radical **R2** introduces a methyl branch (MB) defect in the polymer chain. This mechanism was originally suggested by Rigo and was proven to be the main route to the formation of MB in PVC.[24,25] Alternatively, the radical **R2** can also be involved in a Cl abstraction by the monomer (**Bf**), forming an allylic end group (EA). The radical **R2** can also undergo a second Cl shift (**Bc**) to produce the radical **R3**. Further propagation leads to an ethyl branch (EB) on the polymer backbone (**Bh**) or a Cl abstraction by the monomer (**Bg**) again leads to allylic end groups (EA). For the reactions **Be** and **Bh** an additional parameter *m* is introduced to evaluate the chain length dependence of propagation to an anomalous radical.

Reaction Class C: Backbiting. The second competitive reaction scheme is the intramolecular H shift or backbiting (Scheme 3) which gives rise to butyl branches (BB), pentyl branches (PB), internal allylic chlorines (IA) and diethyl branches (DEB). The growing radical abstracts a H atom from the 5th or the 6th carbon atom on its backbone trough a cyclic transition state (reactions **Ca** and **Cb**). Further propagation of the new radical center gives rise to butyl branches (BB) and pentyl branches (PB) respectively (**Cc** and **Cf**). For instance **Cc_3_1** is the first addition of VC to the radical formed after 1,5 backbiting of a living polymer with 3 monomer units. The radical formed after 1,5 backbiting is also the precursor for the formation of diethyl branches (DEB). In this reaction mechanism the radical undergoes only one VC addition (**Cd**) which is followed by an intramolecular H-transfer (**Cg**) before further propagation (**Ch**). The radical formed after 1,6 backbiting can also undergo a Cl abstraction reaction by the monomer (**Ce** or **Ce′**), generating internal double bonds in the polymer chain (IA).

Reaction Class D: Transfer to Polymer. The living radical in Scheme 1 can be involved in intermolecular H-transfer reactions (transfer to polymer) with the dead polymer (Scheme 4), and this leads to long chain branches with tertiary Cl or tertiary H (LCB and LCB′) and IA. Similar reactions with the typical end groups LE and LE′ have been proposed as an alternative source of methyl branches MB and as an origin of methyl branches containing tertiary chlorine (MB′). H abstraction from a midchain CHCl or CH_2 site (**Da** and **Db** respectively) followed by propagation (**De** and **Df**) introduce long chain branches with tertiary chlorine (LCB) or with tertiary hydrogen (LCB′). As in previous reaction schemes radicals of the type −CH*−CHCl− can undergo a Cl abstraction by the monomer (**Dg**), forming an internal double bond in the polymer chain (IA). Note that in this scheme the midchain position of H abstraction is defined by giving the number of monomer units to the left (n_1) and to the right (n_2), where the total number of monomer units amounts to $n = n_1 + n_2 + 1$. The abstraction reaction in this case is written as **Dt_n$_1$_n$_2$** with **t** = a or b. H abstraction from a CH_2 site of a LE chain end (**Dc**) with subsequent propagation (**Dh**) is an alternative mechanism for the formation of methyl branches (MB), while H abstraction from the CHCl site of a LE′ chain end (**Dd**) with subsequent propagation (**Di**) leads to the formation of methyl branches with tertiary Cl (MB′).

Scheme 3. Reaction Class C: Intramolecular H-Transfer (Backbiting)[9,40]

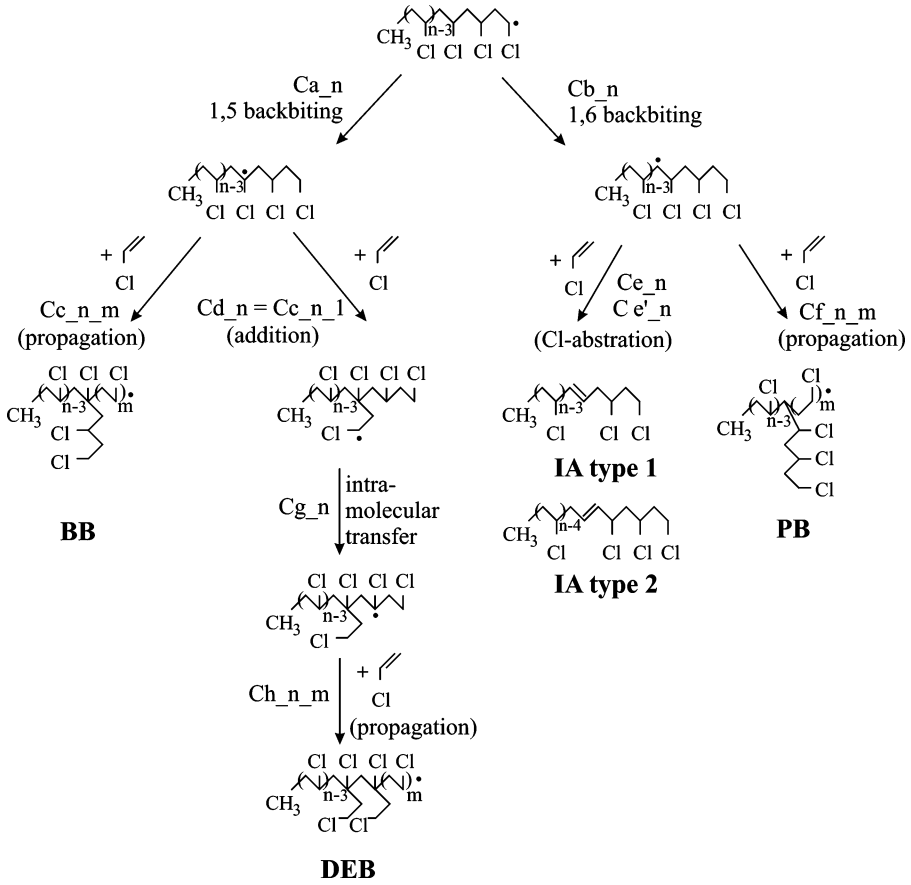

Scheme 4. Reaction Class D: Intermolecular H-Transfer (Transfer to Polymer)[7,9]

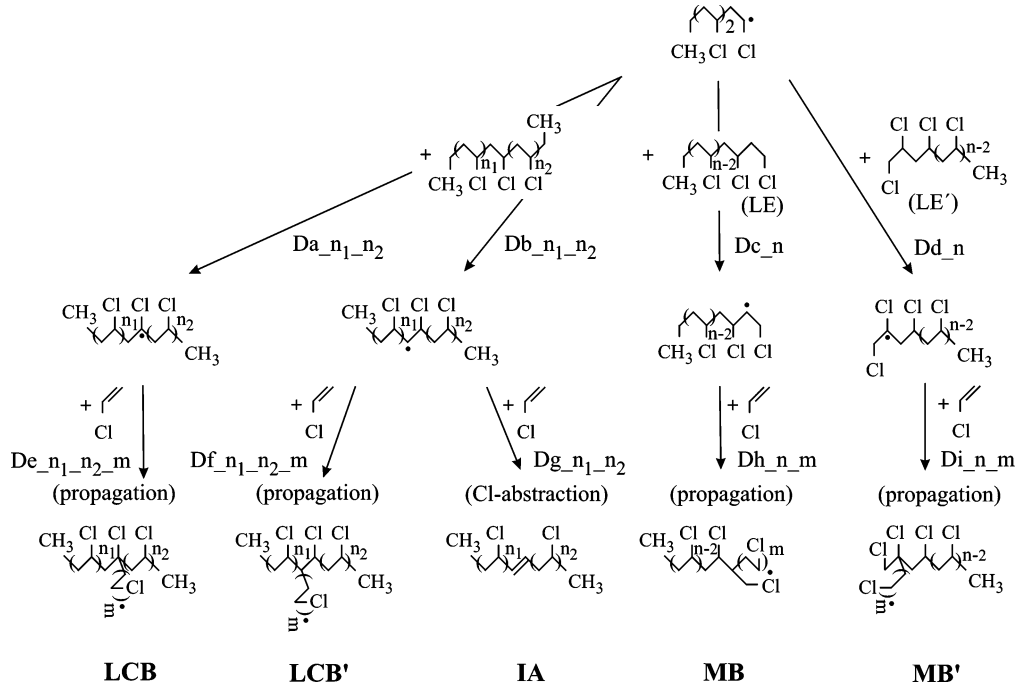

Reaction Class E: Transfer to Monomer. The chain transfer constant to monomer in the polymerization of VC is very high compared to other polymers such as MMA.[26] Thus, this process plays an important role in determining the molecular weight and chain end structure of PVC. The Cl abstractions appearing in reaction classes B, C, and D give rise to a 1,2-dichloro-ethyl radical (Scheme 5). This reaction is the predominant mechanism of chain transfer to monomer during PVC polymerization and leads to an LE′ chain end after propagation (**Ee**).

However in literature some other chain transfer reactions to monomer have been suggested.[2] H or Cl abstractions by the growing radical from the head-side of the monomer (**Ea** and **Eb**), H abstractions from the tail-side of VC (**Ec**), and finally a H transfer to VC from the CH_2 site near the radical center in the growing radical (**Ed**). The H abstraction reactions **Ea** and

Scheme 5. Reaction Class E: Transfer to Monomer[2,3,7]

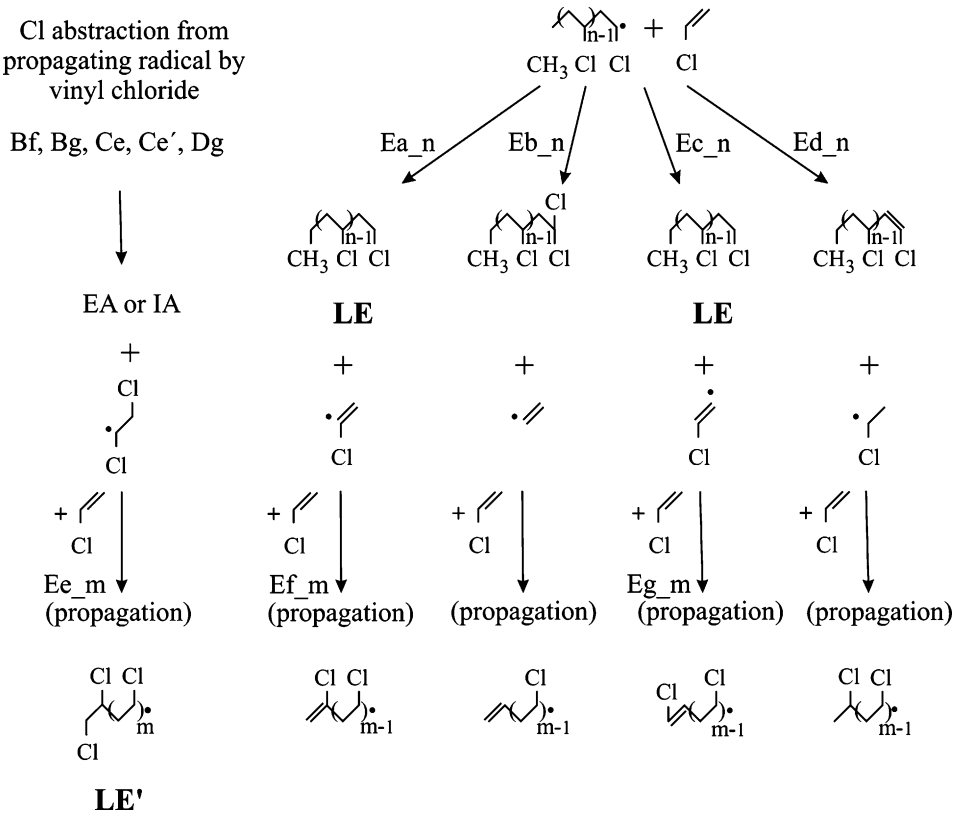

Ec lead to a dead polymer with an LE chain end. The Cl abstraction **Eb** produces a 1,1-dichloroalkane end group and reaction **Ed** introduces a 1-chloro-1-alkene end group on the polymer chain. Further propagation reactions from the radical structures derived from VC leads to living polymer chains with different end groups with minor relevance, since they have not been mentioned in literature. This is an indication that the alternative mechanisms in Scheme 5 are of negligible importance for the chain transfer to monomer, as will also be validated by our ab initio data.

3. Methodology

Reaction Kinetics. Within transition state theory (TST) the rate constant of a uni- and bimolecular reaction (A → B and A + B → C) is related to molecular properties of the reacting specie(s):[27,28]

$$k(T) = \frac{k_B T}{h}\frac{q_{\ddagger}/V}{q_A/V}\mathrm{e}^{-(\Delta E_0/k_B T)},$$

$$k(T) = \frac{k_B T}{h}\frac{(q_{\ddagger}/V)}{(q_A/V)(q_B/V)}\mathrm{e}^{-(\Delta E_0/k_B T)} \quad (1)$$

k_B represents Boltzmann's constant, T the absolute temperature, h Planck's constant, and V the reference volume in which the translational part of the partition function is evaluated. The molecular partition functions q_A and q_B relate to the two reactants, and $q_{\ddagger}$ is the molecular partition function of the transition state. ΔE_0 represents the molecular energy difference at absolute zero between the activated complex and the reactant(s), with inclusion of the zero point vibrational energies.

The molecular properties, such as geometries, ground state energies and frequencies, that are required for the evaluation of the partition functions, and the reaction barrier ΔE_0 are obtained by ab initio molecular calculations. The kinetic parameters are deduced from fitting the results of the TST expression to the Arrhenius rate law in a specific temperature range:

$$k(T) = A\mathrm{e}^{-E_a/RT} \quad (2)$$

In our case, the temperature range of experimental relevance is 320−350 K. Comparison of the TST expression with the Arrhenius rate law shows that the pre-exponential factor A is largely determined by the molecular partition functions, while the molecular energy difference ΔE_0 is a first order approximation for the activation energy E_a.

Computational Details. All calculations are carried out with the Gaussian 03 software package.[29] The geometry optimizations are performed on the B3LYP/6-31+G(d) level of theory whereas single point calculations are performed with the new BMK method optimized for kinetics.[30] There is a general consensus that B3LYP methods provide an excellent low-cost performance for structure optimizations.[31] For energy predictions, however, B3LYP is less accurate and the use of other more advanced functionals with a more reliable performance for reaction energies is desirable. Recent studies have shown that the new hybrid meta-GGA-functional such as BMK (Boese−Martin for kinetics) performs much better with an overall accuracy of maximum 8 kJ/mol for the barriers heights.[30] The combination of a high percentage of Hartree−Fock exchange with terms dependent on the kinetic energy density in the functional is the origin of the surprisingly good performance of BMK. BMK can actually be considered as a reliable general-purpose functional whose domain of applicability has been expanded to cover transition states without losing its accuracy for geometry optimizations. A lot of recent studies confirm these findings.[32] Consequently, in this work the two-component method BMK/6-311+G(3fd,2p)//B3LYP/6-31+G(d) will be systematically used in all calculations. All stationary points were localized by

Table 2. Concentration of Monomer, Radical and Polymer in mol/m^3 in the Monomer (MP) and Polymer (PP) Phase during the Suspension Polymerization of Vinyl Chloride at Conversions below the Critical Conversion[33]

	MP	PP
monomer	13400	4020
radical	10^{-5}	3×10^{-4}
polymer	0	10

full geometry optimizations. The transition states were verified to have only one imaginary frequency corresponding to the reaction coordinate.

It is well-known that PVC chains can adopt several conformations of similar energy. To identify all those conformations would be a very time-consuming task within the context of this work, due to the large number of reaction paths under study and the substantial chain lengths involved. For instance a chain with 10 internal rotations would require the calculation of 10 one-dimensional rotational potentials. In addition the coupling of each internal rotor with its nearest neighbors must be considered. This procedure has been outlined in detail in a previous publication of the authors concerning the propagation of polyethylene.[20] In the present work we studied approximately 100 reactions and a full conformational search would require about 2000 rotational potentials. However the conformations have been chosen on a systematic basis based on stereoelectronic arguments, we always used the extended (all trans) syndiotactic conformation of the PVC radical chains involved. In the study of Izgorodina and Coote, a conformational search indeed revealed that this type of conformation was the global energy minimum for the linear PVC chains containing up to three monomer units.[19]

Calculation of Defect Concentrations. Rate constants of unimolecular reactions (e.g., backbiting or Cl shift) and bimolecular reactions (e.g., propagation and chain transfer) cannot be directly compared as they have different units. To circumvent this problem modified rate constants are introduced for bimolecular reactions, by multiplication with the concentration of one of the reactants:

$$\frac{dc_{\text{product}}}{dt} = k(T)c_A c_B = k'(T)c_A \qquad (3)$$

For the propagation reactions and chain transfer reactions to monomer, reactant B is the vinyl chloride monomer while for the chain transfer reactions to polymer, reactant B represents the dead polymer chain. These concentrations can be obtained by a macroscopic kinetic model of the PVC polymerization and are shown in Table 2.[33] At a temperature of 330 K, the concentration of the monomer amounts to 13400 mol/m^3 in the monomer phase (MP) and 4020 mol/m^3 in the polymer phase (PP,30 wt % VC).[33] These values are valid for the monomer conversion range during which both phases coexist. At a conversion of about 70%, the monomer phase disappears and the monomer concentration in the polymer phase starts to drop. The concentration of radicals is 10^{-5} mol/m^3 in the monomer phase and 3×10^{-4} mol/m^3 in the polymer phase.[33] Finally the polymer concentration in the polymer phase is about 10 mol/m^3. A typical polymeric chain contains about 1000 VC units, so the concentration of polymerized VC in the polymer phase amounts to 10^4 mol/m^3. This concentration can be directly determined from the density of poly(vinyl chloride), which is about 1.4 g/cm^3.[10,33] The polymer concentration is zero in the monomer phase since the solubility of PVC in its own monomer is about 0.03% at ambient temperature and is also limited to polymer chains containing 10 monomer units or fewer.[33]

The defect concentrations are obtained by dividing the rate of formation of the defect by the head-to-tail propagation rate, i.e., the reference reaction leading to a perfect PVC structure. This procedure has been applied by Gilbert et al. for the calculation of the butyl branch (BB) concentration in polyethylene.[17] An analogous approach can be followed for the defects formed in Schemes 2−5. The concentration of the reactive intermediates that appear in the rates of formation of the modeled defects can be eliminated by the hypothesis of the pseudo steady state (PSS). This is illustrated for the MB concentration in the Supporting Information. The PSS hypothesis implies that the concentrations of the reactive intermediates are supposed to be very small and the time derivatives of the concentrations of the reaction-intermediates are set to zero. The derived formula for the theoretical relative defect concentrations can be found in the Supporting Information. The rate coefficient of the reference propagation reaction (**Aa**) that figures in the denominator of the formulas is also calculated on theoretical basis, rather than using the experimental propagation rate. This approach gives the best results since the relative kinetic parameters are supposed to be well predicted with the selected cost-effective method due to the cancellation of systematic errors.

4. Results and Discussion

In this section the ab initio kinetic parameters and the derived ab initio defect concentrations are discussed for the investigated reaction mechanisms. Table 3 summarizes all kinetic data for a chain length of three monomer units. For reaction class C, the data for $n = 4$ are listed since this is the minimum chain length to model the backbiting reactions realistically and those values were used for the calculation of the defect structures arising from this reaction class. The extensive data for each reaction class—with varying chain lengths—are given as Supporting Information in Tables S1−S5.

The head-to-tail propagation serves as a reference for the kinetics of all other elementary reactions leading to anomalous structures in PVC. The kinetic parameters of the addition with a radical consisting of three monomeric units are used throughout this paper. The corresponding transition state is shown in Figure 1 (tsAa_3). The theoretical activation energy for propagation is about 33 kJ/mol. The activation energies, determined by experimental data fitting to a macroscopic kinetic model vary between 23 and 28 kJ/mol.[10−12] The theoretical estimate is within the accuracy limit of 8 kJ/mol of the used BMK functional. For the experimental values of the propagation rate coefficient, values are reported that differ over an order of magnitude: ref 10 reports a value of about 1.1 m^3 mol^{-1} s^{-1} at 330 K while in ref 9 a value of 12 m^3 mol^{-1} s^{-1} is given. Our theoretical estimate of 0.052 m^3 mol^{-1} s^{-1} underestimates these values due to the overestimation of the activation energy. As our primary goal consists in predicting the relative probabilities of the different reaction routes leading to structural defects rather than in reproducing the experimental rate constants, the applied methodology is sufficient to produce theoretical estimates of the concentration of structural defects that are quantitatively relevant.

A head-to-head (HH) addition (reaction **Ba**, Scheme 2) is disfavored over a head-to-tail (HT) addition as the stability of the resulting radical is much lower. In the addition product of a HT addition, the free radical is located on the head end and the substituent is able to provide stabilization by an inductive effect. Bond dissociation enthalpy (BDE) values are a good measure for the stability of the formed radical. In this case the

Table 3. Kinetic Parameters Fitted in the Temperature Range 270-400 K of the Studied Reactions with a Chain Length of Three Monomer Units (Except for the Backbiting Reactions—Class C—Where the Values for $n = 4$ Are Given)[a]

reaction	ΔE_0, kJ/mol	A, $m^3 mol^{-1}$ s^{-1} or s^{-1}	E_a, kJ/mol	k_{330K}, $m^3 mol^{-1} s^{-1}$ or s^{-1}	k'^{MP}_{330K}, s^{-1}	k'^{PP}_{330K}, s^{-1}
Aa_3	28.52	4.82E+03	32.69	3.17E−02	4.24E+02	1.27E+02
Ba_3	39.52	1.34E+03	43.37	1.80E−04	2.41E+00	7.24E−01
Bb_3	50.51	1.85E+13	51.86	1.14E+05		
Bc_3	51.70	1.71E+13	53.24	6.38E+04		
Bd_3	47.84	1.14E+13	49.40	1.73E+05		
Be_3_1	29.73	2.26E+03	33.70	1.03E−02	1.38E+02	4.15E+01
Bf_3	45.91	7.08E+05	52.79	3.06E−03	4.10E+01	1.23E+01
Bg_3	49.79	6.20E+05	56.70	6.45E−04	8.64E+00	2.59E+00
Bh_3_1	38.12	5.73E+02	41.99	1.27E−04	1.70E+00	5.10E−01
Ca_4	73.24	2.68E+11	72.78	8.09E−01		
Cb_4	100.20	1.62E+11	99.59	2.80E−05		
Cc_4_1	38.60	2.29E+02	42.83	3.73E−05	5.00E−01	1.50E−01
Cc_4_2	32.21	2.35E+03	36.21	4.28E−03	5.73E+01	1.72E+01
Cd_4 = Cc_4_1	38.60	2.29E+02	42.83	3.73E−05	5.00E−01	1.50E−01
Ce_4	53.34	1.50E+06	61.11	3.12E−04	4.18E+00	1.25E+00
Ce'_4	50.76	2.29E+06	58.65	1.17E−03	1.56E+01	4.69E+00
Cf_4_1	49.58	2.65E+02	52.64	1.21E−06	1.63E−02	4.88E−03
Cg_4	77.00	3.64E+11	76.37	2.98E−01		
Da_1_1	65.04	9.51E+02	70.08	7.55E−09		7.55E−05
Db_1_1	57.15	6.04E+02	62.01	9.05E−08		9.05E−04
Dc_3	56.31	1.25E+03	61.14	2.57E−07		
Dd_3	56.02	2.14E+02	60.71	5.17E−08		
De_1_1_1	32.51	5.89E+02	36.81	8.62E−04		3.46E+00
Df_1_1_1	41.30	4.00E+02	44.85	3.13E−05		1.26E−01
Dg_1_1	56.39	2.66E+06	63.06	2.73E−04		1.10E+00
Dh_3_1 = Be_3_1	29.73	2.26E+03	33.70	1.03E−02		4.15E+01
Di_3_1	31.65	3.87E+02	35.71	8.44E−04		3.39E+00
E_a_3	69.82	2.24E+04	75.16	2.77E−08	3.72E−04	1.11E−04
Eb_3	107.95	5.34E+04	114.43	4.02E−14	5.39E−10	1.62E−10
Ec_3	79.32	2.85E+04	84.82	1.05E−09	1.40E−05	4.20E−06
Ed_3	118.43	8.54E+03	123.58	2.29E−16	3.07E−12	9.21E−13
Ee_3	23.22	5.39E+03	27.68	2.20E−01	2.95E+03	8.85E+02
Ef_3	24.36	5.56E+03	28.51	1.68E−01	2.24E+03	6.73E+02
Eg_3	24.17	7.94E+03	28.38	2.51E−01	3.37E+03	1.01E+03

[a] For the bimolecular reactions also the modified reaction rate constant k' is given in the monomer and the polymer rich phase.

HT and HH product radicals are characterized by a BDE of 403.31 and 420.20 kJ/mol, respectively. These values were obtained at the BMK/6-311+G(3df,2p)//B3LYP/6-31G+(D) level which was recommended by some of the present authors in ref 34 as a result of an extended level of theory study. Following the Evans−Polanyi−Semenov relation,[35] the activation energy of the HH addition is about 10 kJ/mol higher than a HT addition. The rare event of a head-to-head addition (rate-determining step in Scheme 2) has however a large impact since it initiates a cascade of reactions that have been proven to be the main reaction routes to the formation of some short branches and typical end group structures. The head-to-head radical will rearrange itself very quickly to the more stable secondary radical through the very fast Cl shift reaction **Bb** (Figure 1, tsBb_3). Indeed our calculated rate constants reflect this tendency, the first Cl shift is about 3 orders of magnitude faster than the reference HT propagation. Recall that the rate constant of this unimolecular reaction must be compared with the modified rate constant k' of the bimolecular addition. The modified rate constant is given in the monomer phase (MP) as well as in the polymer phase (PP). The first Cl shift **Bb** is exothermic, i.e., characterized by a reaction enthalpy at 298.15 K of −17.3 kJ/mol at the B3LYP/6-31+G(d) level of theory and is not reversible. The second Cl shift **Bc** is reversible—characterized by a reaction enthalpy of ≈0—as it concerns the rearrangement between secondary radicals (reaction **Bd**).

Further propagation (**Be**) after the first Cl shift leads to the formation of a methyl branch (MB) and this is the main reaction route toward this defect structure. The kinetic parameters of the latter addition were modeled in terms of varying chain length, i.e., by varying the parameter m and the results are taken up in Table S2 of the Supporting Information. The barriers vary around 33 kJ/mol which is very close to the values of the normal H−T propagation (Table S1). Vinyl chloride (VC) can also add to the radical **R3**, which is formed after the second Cl shift, leading to an ethyl branch (EB). This addition (**Bh**) is higher activated as the radical site on the polymer backbone is less accessible which is reflected in the rate constant that is 2 orders of magnitude lower. Therefore, the number of MB defects will be larger than the number of EB defects, which is in correspondence with literature (Table 1).

For both the radicals **R2** and **R3** addition or Cl abstraction with the VC monomer (**Bf** and **Bg**) are competitive reaction routes and the relative rates determine the final number of MB and EB defect structures with respect to EA defects. In ref 8, it was shown that the numerical ratios for (addition to VC)/(Cl abstraction by VC) must be the same for radicals **R2** and **R3**. This is not the case for our ab initio rate constants and this can be attributed to the higher activation energy of addition (**Bh**) as indicated above. The transition state for Cl abstraction is visualized in Figure 1 (tsBf_3). For the Cl abstraction reactions with VC, a refinement of our theoretical treatment was introduced due to the observation that the transition state normal mode spectrum contains one very low frequency, corresponding to the internal rotation of VC about the forming/breaking bond. In the case of reaction **Bf_3** the frequency amounts to 7.6 cm^{-1} and the harmonic oscillator model is inappropriate for obtaining reliable partition functions.[36] For the Cl abstraction a mixed harmonic oscillator/free rotor (HO/FR) model is used in which all internal motions except the rotation about the forming/breaking bond are treated in the harmonic oscillator model. In the case of reaction **Bf_3**, this theoretical refinement leads to a

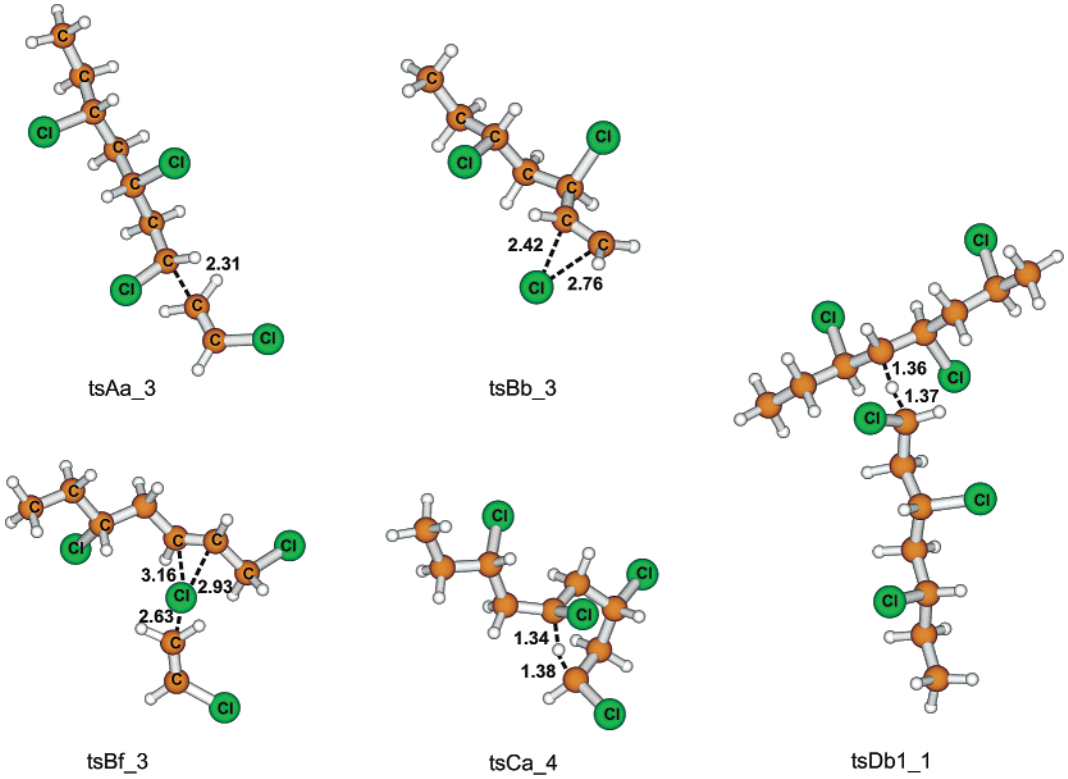

Figure 1. Optimized structure at B3LYP/6-31+G(d) of some key reactions: the transition state of the propagation **tsAa_3**, of the first Cl shift **tsBb_3**, of a Cl abstraction with the monomer **tsBf_3**, of the 1,5 backbiting **tsCa_4**, and of an intermolecular H shift **tsDb_1_1**. The indicated distances are in angströms (Å).

Table 4. Experimental and Theoretical Concentrations of Structural Defects in PVC, in Number Per 1000 VC Units[a]

type defect	exptl no.	*B*	*C*	*D*	*E*	calcd no.
MB	3.3−4.8	4.3		<1.6E−9		4.3
BB	0.5−1.7		0.14			0.14
EA	0.45−0.95[b]	1.4 (1.0[b])				1.4 (1.0[b])
LE'	0.8−0.9[b]				1.4 (1.0[b])	1.4 (1.0[b])
EB	0.14−0.55	0.020				0.020
IA	0.0−0.6		4.7E−6	6.4E−3		6.4E−3
LCB	0.07−0.14			5.9E−4		5.9E−4
LCB′	0.03−0.07			7.3E−4		7.3E−4
LE	<0.75				9.1E−4	9.1E−4
DEB	ND		6.9E−5			6.9E−5
MB'	ND			3.3E−10		3.3E−10
PB	ND		3.8E−9			3.8E−9

[a] $n = 3$, except for reaction class C (backbiting, $n = 4$). [b] The experimental concentrations of the end group structures EA and LE′ are expressed in number per molecule. (ND = Not Detected.)

reduction of the rate constant by a factor three in the temperature range of relevance. Moreover the Cl abstractions are higher activated than the additions ($E_a = 34$ kJ/mol for Be_3_1 compared to $E_a = 53$ kJ/mol for Bf_3). Finally the rate of the addition reaction Be_3_1 is about three times larger than that of the Cl abstraction reaction Bf_3. The competition between these reaction routes is reflected in the defect concentrations of methyl branches (MB) and allylic end groups (EA). The absolute values are taken up in column B of Table 4. The theoretical number of methyl branches is 4.3, while the experimental range is 3.3−4.8. This excellent agreement confirms that reaction scheme *B* is the dominant route for the production of the most abundant branch structure MB in PVC. The number of allylic end groups (EA) amounts to 1.4, which is about a factor three lower than the MB branches. Remark that the experimental EA concentration is expressed in number per molecule, so we need to convert the calculated concentration (in number per 1000 VC) via the following equation: number per chain = (number per 1000 VC * average degree of polymerization)/1000.[9] Taking into account an average degree of polymerization of about 740 at 55 °C in commercial suspension PVC[37], the theoretical number of EA defects is about 1.0 per molecule. The experimental concentration of both defects and thus their relative abundance is predicted correctly. The number of ethyl branches r_{EB} underestimates the experimental range, but the relative order of abundance (MB > EA > EB) is in correspondence with experiment.

To illustrate the failure of the B3LYP/6-31+G(d) method in predicting the relative probabilities of the reactions in class B, the kinetic parameters are given in Table S6 of the Supporting Information. The Cl shift and Cl abstraction reactions are not correctly described.

The transition state for a typical 1,5 backbiting is shown in Figure 1 (tsCa_4). It concerns an intramolecular H shift that proceeds via a six-membered transition state. The kinetics are modeled in terms of varying chain length and the results are given in Table S3 of the Supporting Information. As already mentioned, we use the data for $n = 4$ for the calculation of defect concentrations, since this is the minimum chain length to model the backbiting reactions realistically (cf. Scheme 3). The 1,6 backbiting occurs via a seven-membered transition state and is therefore expected to be higher activated.[38] Both backbiting steps (**Ca** and **Cb**) are relatively highly activated compared to the normal HT propagation but the 1,5 backbiting is strongly preferred over the 1,6 backbiting. This is reflected in both the activation energies ($E_a^{Ca} - E_a^{Cb} \simeq 27$ kJ/mol, $n = 4$) and the rate constants ($k_{Ca}/k_{Cb} \simeq 3 \times 10^4$, $n = 4$). Toh et al. found a similar value for the activation energy of an 1,5 backbiting during polyethylene propagation (66.9 kJ/mol, QCISDT/6-311g**).[17] Since these reactions are the rate-determining steps for the formation of BB and PB in Scheme

3, the PB concentration will be negligible in agreement with the experimental findings. The propagation steps **Cc** following the 1,5 backbiting converge rapidly to the kinetic parameters of **Aa**. The first monomer addition to the midchain radical (**Cd** = **Cc_1**) has an activation energy that is substantially higher than that of the normal propagation (43 kJ/mol instead of 33 kJ/mol). Instead of further propagation after the first VC addition (**Cd_n** = **Cc_n_1**), the pendent radical 1-chloro-eth-1-yl group can abstract a H atom from an adjacent CHCl group on the main chain (reaction **Cg**). These reactions have similar transition states as the first 1,5 backbiting reaction of Scheme 3 and are likewise highly activated (E_a = 76 kJ/mol, n = 4). Further propagation (**Ch**) after this slow reaction step would introduce a diethyl branch (DEB) in the polymer. As the formation of DEB defects needs two very slow reaction steps (**Ca** and **Cg**), its concentration is expected to be very low. This is indeed reflected in the quantitative value of the DEB concentration, i.e., 6.9 E-5 (Table 4, column C). According to Starnes, the DEB structure can only occur at significant levels in industrial PVC fractions that are made at very high VC conversions.[7] The presence of diethyl branches was demonstrated from ^{13}C NMR on a PVC sample that was made at subsaturation conditions.

Within reaction class C, we also investigate the possible reaction paths following 1,6 backbiting. The radical can undergo either an addition (**Cf**) or a Cl abstraction (**Ce** or **Ce′**), which are two competitive pathways as already introduced in reaction class B. As the 1,6 backbiting has a rate constant which is 4 orders of magnitude smaller than the 1,5 backbiting, we expect low concentrations for the corresponding defect structures. The internal double bonds (IA) formed via Scheme 3 will thus give a minor contribution to the total IA content in the polymer. Quantitative values for the defect concentrations are given in column C of Table 4. The concentration of BB is about 0.14 per 1000 monomeric units, which underestimates the experimental value (0.5−1.7/1000 VC). The latter defect is important for the thermal instability, due to the presence of tertiary Cl. The number of DEB is below the detection limit of 0.1/1000 VC, which is in accordance with experiment. The number of internal bonds formed after 1,6 backbiting (**Cb**) is very low (4.7×10^{-6} /1000 VC) since this reaction is highly activated and it only gives a minor contribution to the total internal double bond content (0.0−0.6/1000 VC). The major contribution to internal allylic bonds is formed as a result of reactions appearing in reaction class D (see discussion below). Finally the number of PB is also verly low (3.8×10^{-9} /1000 VC), which is in agreement with the lack of experimental evidence for this type of defect.

Reaction class D groups all reactions following a transfer to polymer, in which a living polymer abstracts a H atom from a dead polymer segment. The living radical polymer is modeled by a chain with three monomer units added to a methyl radical. In all cases the transfer reaction (**Da**−**Db**−**Dc**−**Dd**) is the rate-determining step in the reaction sequences. The kinetic data for the transfer reactions to polymer (Scheme 4) are given in Table 3 for n = 3. The extensive data are listed in Table S4 of the Supporting Information.

For the formation of the long chain branches and internal allylic bonds, the abstraction of the living polymer occurs at a random midchain position in the dead polymer. The latter is modeled by a regular chain with $n_1 + n_2 + 1$ monomer units, terminated by two methyl groups (cf. Scheme 4). The hydrogen can be abstracted either at a CH_2 or CHCl site. The transition states for the abstraction at the CH_2 site is shown in Figure 1 (tsDb_1_1). As for the Cl abstractions, the transition state is also characterized by a very low-frequency mode, corresponding to the rotation about the forming/breaking bond. Likewise the mixed HO/FR approximation was used for these class of reactions. The abstraction at the CH_2 site is preferred, with a difference in activation energy of about 8 kJ/mol (E_a = 70 kJ/mol for Da_1_1 compared to 62 kJ/mol for Db_1_1). The preference must be traced back to specific unfavorable energetic effects in the transition state when two CHCl groups approach to abstract the hydrogen from the dead polymer.

Similarly as in the backbiting scheme, the −CCl*− radical can further propagate whereas the −CH*− radical can either undergo a propagation or Cl abstraction. The defects formed after further propagation are long chain branches. From previous discussions it can be expected that the propagation will be faster than the Cl abstraction, which is indeed reflected in the activation energies, i.e., E_a = 45 kJ/mol for **Df** compared to 63 kJ/mol for **Dg**. The right side of Scheme 4 are alternative pathways for the formation of methyl branches. In these cases a hydrogen is abstracted at the CH_2 site of a chain end of type 1,3-dichloroalkane (LE) or at the CHCl site of a chain end of type 1,2-dichloroalkane (LE′). Both chain ends are formed in reaction class E, that concerns the transfer to monomer. As for the midchain case, abstraction at the CH_2 site is preferred. Anyway both abstractions are relatively slow, characterized by reaction barriers of about 61 kJ/mol. The contribution of these reaction steps to the formation of methyl branches is negligible, as the rate-determining step of this scheme, i.e., the initial hydrogen abstraction is much higher activated than the rate-determining step in Scheme 2, i.e., the head to head addition. Furthermore, the reactants for **Dc** and **Dd** are defect structures (LE and LE′) which concentrations are very low in contrast to the monomer concentration. These results are in accordance with Purmova et al.[9] In conditions of monomer starvation however this mechanism can become competitive with the methyl branch formation in Scheme 2. For the calculation of the defect concentrations in reaction class D, the typical concentrations of monomer and polymer in the polymer-rich phase were used. The defect concentrations are given in column D of Table 4. The concentration of LCB, LCB′, and IA are all underestimated with respect to the experiment. This discrepancy seems to be originating in the low theoretical predictions for the frequency factor of the H abstraction reactions in Scheme 4. H abstraction reactions with a long chain are studied and it is not a priory clear what repercussions this has on the pre-exponential factor. To unravel the origin of the low pre-exponential factor a thorough theoretical study would be advisable in which the effect of bending modes, internal rotations etc. needs to be taken into account. The number of methyl branches with tertiary Cl (MB′) is very low (below the detection limit) which is in correspondence with experiment. The contribution of reaction class D to the methyl branch concentration is negligible as anticipated before.

Finally the kinetic parameters for the transfer reactions to monomer are discussed. The main mechanism of transfer to monomer is the Cl abstraction by VC figuring in Scheme 2 (**Bf**, **Bg**). However, the auxiliary routes in Scheme 3 and 4 are even more important since they give rise to the thermally instable IA defect (**Ce**, **Ce′**, **Dg**).[3] More details about this auxiliary mechanism for transfer to monomer during vinyl chloride polymerization and its implications for the thermal stablility is given in ref 8. The 1,2-dichloroethyl radical that is formed after a Cl abstraction can undergo subsequent propagations (**Ee**). This is illustrated in Scheme 5, together with the alternative mechanisms of transfer to monomer as suggested

by Endo.[2] The kinetic data for $n = 3$ are given in Table 3 whereas for other chain lengths the kinetics is summarized in Table S5 of the Supporting Information. All alternative pathways proposed by Endo (**Ea**, **Eb**, **Ec**, and **Ed**) are much higher activated than the Cl abstractions (**Bf**, **Bg**) occurring in Scheme 2 and might be expected to give negligible contributions to the chain transfer. Comparison among the alternative reaction mechanisms learns that **Eb** and **Ed** are extremely high activated and therefore we did not calculate the subsequent propagation reactions. The reactions **Ea** and **Ec** introduce a LE end group in the polymer chain. The subsequent propagation steps (**Ef** and **Eg**) are very fast due to the occurrence of the vinylic type of radicals.

The defect concentrations corresponding to reaction class E are listed in column E of Table 4. The 1,2-dichloroethyl radical in Scheme 5 is formed by Cl abstraction from several reaction classes (B, C, and D). The total number of LE′ end groups formed after the propagation steps **Ee** is 1.4 per 1000 VC and is mainly formed by reaction scheme B as generally accepted in literature (dominant mechanism of transfer to monomer). As for the EA structure in class B, the experimental LE′ concentration is expressed in number per molecule. Conversion to the number per 1000 VC (taking into account an average degree of polymerization of about 740) leads to an experimental range of 1.0−1.2/1000 VC. Our theoretical value of 1.4/1000 VC is in good agreement with the experimental value. The number of LE chain ends formed by reactions **Ea** and **Ec** is about 9×10^{-4} per 1000 monomer units, far below the detection limit of 0.1/1000 VC. It must be noticed however that the defect structure LE is also formed in the case of termination by disproportionation.

5. Conclusions

In this work, an ab initio study on the BMK/6-311+G(3df,2p)//B3LYP/6-31+G(d) level of theory was performed on the currently accepted reaction mechanisms for the formation of structural defects in PVC at monomer conversions below 85%. The chain length dependence was taken into account by varying the chain length of the propagating radical as well by modeling subsequent propagation steps on the irregular radical structures leading to the formation of defects. The total number of elementary steps calculated on an ab initio basis amounts to 32, but the variation of the chain length led to more than 100 studied reactions. The head-to-tail propagation was calculated as a reference reaction to measure the probability of the side reactions that introduce structural defects. More specifically it concerns the reactions following head-to-head propagation, the backbiting reaction mechanism (intramolecular H abstraction), and the transfer reactions to polymer and monomer. Quantitative values for the defect concentrations were generated by combination of the hypothesis of the pseudo steady state for the concentration of the reactive intermediates in the reaction schemes combined with typical monomer, radical and polymer concentrations during PVC suspension polymerization. In all reaction schemes the first step is rate determining, making a simple classification by probability of occurrence possible: head-to-head (1%) > backbiting (0.1%) ≫ H abstraction reactions. The head-to-head scheme is very important since it explains the formation of the most abundant defect structure in PVC, i.e., the methyl branch (MB). The experimental concentration of about 4 MB defects per 1000 VC units was reproduced by the theoretical calculation from the ab initio kinetic parameters. The backbiting reaction mechanism generates the second most abundant branch structure, namely the butyl branch (BB). Its abundance is about 1 per 1000 monomer units. This defect can however be considered more important than the MB structure since it gives a large contribution to the thermal instability due to the presence of the tertiary chlorine at the branch point. For the BB defect, an underestimation of the experimental value was noticed. The intermolecular H abstraction reactions lead to internal double bonds (IA) and long chain branches with tertiary chlorine (LCB). The internal double bond content also contributes to the thermal instability but its concentration is lower than the tertiary chlorine content (approximately 0.1 compared to 1 per 1000 VC). The calculated value is approximately 10 times smaller than the experimental value. The number of LCB values was underestimated by 2 orders of magnitude, however it could be expected a priori that the deviations become larger for the less abundant defect structures, moreover the experimental values are less reliable since they are in the same order of magnitude of the experimental errors. It can be concluded that the ab initio calculations on the presented reaction mechanisms leading to defect formation in PVC lead to an excellent prediction of the experimentally measured concentrations of the most abundant defect structures in PVC. This confirms that the presented reaction mechanisms are indeed the dominant reaction routes to the formation of the studied defect structures for conversions below 85%.

Acknowledgment. This work was supported by the Fund for Scientific Research, Flanders (FWO), and the Fund for Scientific Research of the Ghent University.

Supporting Information Available: Text discussing the determination of the ab initio concentrations of structural defects in terms of the kinetic parameters and Table S1−S5, containing the kinetic parameters at the BMK/6-311+G(3df,2p)//B3LYP/6-31+G(d) level of theory of reaction classes A-E with varying chain length, and Table S6, illustrating the failure of the B3LYP/6-31+G(d) method in predicting the relative probabilities of the propagation reactions compared to the Cl shift and the Cl abstraction reactions for reaction class B (reactions following a head-to-head addition). This material is available free of charge via the Internet at http://pubs.acs.org.

References and Notes

(1) Braun, D. *J. Polym. Sci., Polym. Chem.* **2004**, *42*, 578−586.
(2) Endo, K. *Prog. Polym. Sci.* **2002**, *27*, 2021−2054.
(3) Starnes, W. H., Jr. *Prog. Polym. Sci.* **2002**, *27*, 2133−2170.
(4) Hjertberg, T.; Sörvik, E. M. *Polymer* **1983**, *24*, 673−684.
(5) Rogestedt, M.; Hjertberg, T. *Macromolecules* **1993**, *26*, 60−64.
(6) Xie, T. Y.; Hamielec, A. E.; Rogestedt, M.; Hjertberg, T. *Polymer* **1994**, *35*, 1526−1534.
(7) Starnes, W. H., Jr. *J. Polym. Sci., Polym. Chem.* **2005**, *43*, 2451−2467.
(8) Starnes, W. H., Jr.; Chung, H.; Wojciechowski, B. J.; Skillicorn, D. E.; Benedikt, G. M. *ACS Adv. Chem. Ser.* **1996**, *249*, 3−18.
(9) Purmova, J.; Pauwels, K. F. D.; van Zoelen, W.; Vorenkamp, E. J.; Schouten, A. J.; Coote, M. L. *Macromolecules* **2005**, *38*, 6352−6366.
(10) De Roo, T.; Wieme, J.; Heynderickx, G. J.; Marin, G. B. *Polymer*, **2005**, *46*, 8340−8354.
(11) Krallis, A.; Kotoulas, C.; Papadopoulos, S.; Kiparissides, C.; Bousquet, J.; Bonardi, C. *Ind. Eng. Chem. Res.* **2004**, *43*, 6382−6399.
(12) Sidiropoulou, E.; Kiparissides, C. *J. Macromol. Sci.—Chem.* **1990**, *27*, 257−288. and references therein.
(13) Heuts, J. P. A.; Gilbert, R. G.; Radom, L. *Macromolecules* **1995**, *28*, 8771−8781.
(14) Heuts, J. P. A.; Gilbert, R. G.; Radom, L. *J. Phys. Chem.* **1996**, *100*, 18997−19006.
(15) Coote, M. L.; Radom, L. *Macromolecules* **2004**, *37*, 590−596.
(16) Huang, D. M.; Monteiro, M. J.; Gilbert, R. G. *Macromolecules* **1998**, *31*, 5175−5187.
(17) Toh, J. S. S.; Huang, D. M.; Lovell, P. A.; Gilbert, R. G. *Polymer* **2001**, *42*, 1915−1920.
(18) Thickett, S. C.; Gilbert, R. G. *Polymer* **2004**, *45*, 6993−6999.
(19) Izgorodina, E. I.; Coote, M. L. *Chem. Phys.* **2006**, *324*, 96−110.

(20) Van Cauter, K.; Van Speybroeck, V.; Vansteenkiste, P.; Reyniers, M. F.; Waroquier, M. *ChemPhysChem* **2006**, *7*, 131−140.
(21) Heuts, J. P. A.; Russell, G. T. *Eur. Polym. J.* **2006**, *42*, 3−20.
(22) LLauro-Darricades, M.-F.; Bensemra, N.; Guyot, A.; Pétiaud, R. *Macromolekul. Chem. Macromol. Symp.* **1989**, *29*, 171−184.
(23) Ugelstad, J.; Mork, P. C.; Hansen, F. K.; Kaggerud, K. H.; Ellingsen, T. *Pure Appl. Chem.* **1981**, *53*, 323−363.
(24) Rigo, A.; Talamini, G.; Palma, G. *Makromol. Chem.* **1972**, *153*, 219−228.
(25) Starnes, W. H., Jr.; Schilling, F. C.; Abbås, K. B.; Cais, R. E.; Bovey, F. A. *Macromolecules* **1979**, *12*, 556−562.
(26) Brandrup, J.; Immergent, E. H. In *Polymer handbook*, 2nd ed.; Wiley: New York, 1975.
(27) Laidler, K. J. In *Chemical kinetics*; HarperCollins Publishers, Inc.: New York, 1987.
(28) Mc. Quarrie, D. A.; Simon, J. D. *Physical Chemistry—A molecular approach*; University Science Books: Sausalito, CA, 1997.
(29) Gaussian 03, Revision B.03. Frisch, M. J.; Trucks, G. W.; Schlegel, H. B.; Scuseria, G. E.; Robb, M. A.; Cheeseman, J. R.; Montgomery, J. A., Jr.; Vreven, T.; Kudin, K. N.; Burant, J. C.; Millam, J. M.; Iyengar, S. S.; Tomasi, J.; Barone, V.; Mennucci, B.; Cossi, M.; Scalmani, G.; Rega, N.; Petersson, G. A.; Nakatsuji, H.; Hada, M.; Ehara, M.; Toyota, K.; Fukuda, R.; Hasegawa, J.; Ishida, M.; Nakajima, T.; Honda, Y.; Kitao, O.; Nakai, H.; Klene, M.; Li, X.; Knox, J. E.; Hratchian, H. P.; Cross, J. B.; Bakken, V.; Adamo, C.; Jaramillo, J.; Gomperts, R.; Stratmann, R. E.; Yazyev, O.; Austin, A. J.; Cammi, R.; Pomelli, C.; Ochterski, J. W.; Ayala, P. Y.; Morokuma, K.; Voth, G. A.; Salvador, P.; Dannenberg, J. J.; Zakrzewski, V. G.; Dapprich, S.; Daniels, A. D.; Strain, M. C.; Farkas, O.; Malick, D. K.; Rabuck, A. D.; Raghavachari, K.; Foresman, J. B.; Ortiz, J. V.; Cui, Q.; Baboul, A. G.; Clifford, S.; Cioslowski, J.; Stefanov, B. B.; Liu, G.; Liashenko, A.; Piskorz, P.; Komaromi, I.; Martin, R. L.; Fox, D. J.; Keith, T.; Al-Laham, M. A.; Peng, C. Y.; Nanayakkara, A.; Challacombe, M.; Gill, P. M. W.; Johnson, B.; Chen, W.; Wong, M. W.; Gonzalez, C.; Pople, J. A. Gaussian, Inc.: Wallingford CT, 2004.
(30) Boese, A. D.; Martin, J. M. L. *J. Chem. Phys.* **2004**, *121*, 3405−3416.
(31) Coote, M. L. *J. Phys. Chem. A* **2004**, *108*, 3865−3872.
(32) (a) Wood, G. P. F.; Rauk, A.; Radom, L. *J. Chem. Theory Comput.* **2005**, *1*, 889−899. (b) Miller, D. J.; Smith, D. M.; Chan, B.; Radom, L. *Mol. Phys.* **2006**, *104*, 777−794. (c) Wood, G. P. F.; Moran, D.; Jacob, R.; Radom, L. *J. Phys. Chem. A* **2005**, *109*, 6318−6325. (d) Wood, G. P. F.; Easton, C. J.; Rauk, A.; Davies, M. J.; Radom, L. *J. Phys. Chem. A* **2006**, *110*, 10316−10323. (e) Izgorodina, E. I.; Coote, M. L. *J. Phys. Chem. A* **2006**, *110*, 2486−2492.
(33) Xie, T. Y.; Hamielec, A. E.; Wood, P. E.; Woods, D. R. *Polymer* **1991**, *32*, 537−557.
(34) Van Speybroeck, V.; Marin, G. B.; Waroquier, M. *ChemPhysChem* **2006**, *7*, 2205−2214.
(35) (a) Evans, M. G. *Discuss. Faraday Soc.* **1947**, *2*, 271. (b) Evans, M. G.; Gergely, J.; Seaman, E. C. *J. Polym. Sci.* **1948**, *3*, 866. (c) Evans, M. G.; Polanyi, M. *Trans. Faraday Soc.* **1938**, *34*, 11.
(36) Hemelsoet, K.; Moran, D.; Van Speybroeck, V.; Waroquier, M.; Radom, L. *J. Phys. Chem. A* **2006**, *110*, 8942−8951.
(37) Hjertberg, T.; Sörvik, E.; Wendel, A. *Makromol. Chem.—Rapid Commun.* **1983**, *4*, 175−180.
(38) Beckwith, A. L. J. *Tetrahedron* **1981**, *37*, 3073−3100.
(39) Starnes, W. H., Jr.; Wojciechowski, B. J.; Chung, H.; Benedikt, G. M.; Park, G. S.; Saremi, A. H. *Macromolecules* **1995**, *28*, 945−949.
(40) Starnes, W. H., Jr.; Zaikov, V. G.; Chung, H. T.; Wojciechowski, B. J.; Tran, H. V.; Saylor, K.; Benedikt, G. M. *Macromolecules* **1998**, *31*, 1508−1517.
(41) Guyot, A. *Macromolecules* **1986**, *19*, 1090−1096 and references therein: Guyot, A. *Pure Appl. Chem.* **1985**, *57*, 833. Darricades-Llauro, M. F.; Michel, A.; Guyot, A.; Waton, H.; Petiaud, R.; Pham, Q. T. *J. Macromol. Sci. Chem.* **1986**, *23*, 221.
(42) Starnes, W. H., Jr.; Wojciechowski, B. J.; Velazquez, A.; Benedikt, G. M. *Macromolecules* **1992**, *25*, 3638−3641.

MA062174S